Synthesis of lead chalcogenide nanoparticles in block copolymer micelles: investigation of optical properties and fabrication of 2-D arrays of nanoparticles

Savarimuthu Philip Anthony, Won Joon Cho, Jeong In Lee and Jin Kon Kim*

Received 14th August 2008, Accepted 16th October 2008
First published as an Advance Article on the web 14th November 2008
DOI: 10.1039/b814157f

Narrow band gap PbS and PbSe semiconductor nanocrystals were prepared in the poly(4-vinyl pyridine) core of self assembled polystyrene-*block*-poly(4-vinyl pyridine) copolymer micelles in toluene at room temperature, and characterized by high resolution-transmission electron microscopy and X-ray diffractograms. Optical absorption and photoluminescence (PL) studies of the nanocrystals showed the quantized phenomena. The PL intensity of the PbSe nanocrystals was strongly enhanced, with a slight red shift in the peak position, by treating with aqueous Na_2S solution. Interestingly, the inclusion of ZnS amorphous nanoparticles into the P4VP/PbSe core leads to a large red shift in the peak position, which covers the technologically important range (1.3 to 1.55 μm), with strong enhancement of the emission intensity. We fabricated a monolayer thin film of PbSe nanocrystals by spin coating on a silicon wafer, and it showed similar PL behavior to that in solution.

Introduction

Narrow band gap IV–VI semiconductor nanomaterials, for instance, PbS (0.41 eV) and PbSe (0.27 eV), have recently attracted greater attention because of their unique electronic structures and superior optical properties.[1–3] Lead chalcogenide nanocrystals, compared to most II–VI and III–V semiconductors (ZnSe, CdSe, CdS, InAs), exhibit strong quantum size effects due to the large Bohr radii of both electrons and holes (PbS (18 nm) and PbSe (46 nm)) that lead to a large confinement energy.[4,5] Consequently, the PbS and PbSe nanomaterials have been found to be useful in various applications such as in electronic, optical, optoelectronic and thermoelectric devices and solar cells.[6–13] Electroluminescence devices based on PbS and PbSe nanocrystals were demonstrated recently with a size tunable infrared emission between 1.0 and 2.0 μm and high external quantum efficiencies up to 3%.[1,2,12] The large optical nonlinearity observed in PbS and PbSe due to the strong quantum size effects can be used for optical switching and photonic devices.[14,15] Because of the wide size tunability of the band gap energies of PbS and PbSe, the absorption edges and photoluminescence (PL) bands cover the entire near-infrared (NIR) spectral region up to 3 μm.[16,17] This property of lead chalcogenide nanocrystals is particularly appealing for telecommunication and biological applications, since those applications require materials that luminesce in the range between 1300–1550 nm and 700–900 nm, respectively.[10]

The incorporation of PbS and PbSe nanocrystals into the polymer matrix might be highly desirable for many device applications, such as electroluminescent and optical devices.[1,2,12] This is because the integration of nanocrystals on silicon or any substrate could be easily achieved by spin coating or drop casting of polymers containing the nanocrystals. The integration of PbS and PbSe nanocrystals on a silicon substrate would be interesting for all inorganic light emitting heterojunctions. Recently, a 3-D photonic crystal fabricated from PbSe nanocrystals-dispersed polymer nanocomposite was found to facilitate spontaneous emission for the next generation of near infrared photonic applications.[18] High refractive index PbS/polymer nanocomposites were fabricated from reactive lead-containing precursors and polythiourethane oligomer.[19] The polymer matrix has also been effectively utilized for the size controlled synthesis of PbS nanoparticles.[20–24] Polymer fiber matrices have been also used to synthesize narrow size dispersed PbS nanoparticles.[25,26]

The control of patterning or spatial positioning of nanoparticles on a solid substrate, such as a silicon wafer, is important for successful device applications. This could be realized by incorporating nanoparticles into well defined self assembled block copolymer nanostructures.[27–29] Two different methods can be employed to incorporate the nanocrystals in the block copolymer. One is to mix the pre-synthesized, surface functionalized nanocrystals with block copolymer.[30–32] Here, the favorable interaction of surface functional group with one of the blocks of the block copolymer leads to the selective sequestering of the nanocrystals. The other method is to prepare nanocrystals directly inside the micelles of an amphiphilic block copolymer that contains the appropriate metal salts.[33–35] Several groups report on the preparation of metal sulfide nanoparticles directly in block copolymer micelles.[33–38] We have recently prepared CdSe nanoparticles directly in the core of polystyrene-*block*-poly(4-vinyl pyridine) (PS-P4VP) micelles by heterogeneous reaction at room temperature.[39]

In this paper, we prepared PbS and PbSe nanocrystals directly inside the core of PS-P4VP micelles in toluene at room temperature and characterized them by high resolution-transmission electron microscopy (HR-TEM) and X-ray diffractograms

National Creative Research Center for Block Copolymer Self-Assembly, Department of Chemical Engineering and Polymer Research Institute, Pohang University of Science and Technology, Kyungbuk, 790-784, Korea. E-mail: jkkim@postech.ac.kr

(XRD). Optical absorption and photoluminescence (PL) of the nanocrystals reveals the quantum confinement effect of the nanocrystals. The post treatment (Na_2S treatment or the inclusion of ZnS) of the P4VP/PbSe cores leads to the strong enhancement of the PL intensity with a slight or large red shift in the peak position (1.30–1.41 μm), which is important for telecommunication applications. Finally, we fabricated monolayer thin films of PS-P4VP/PbSe and observed similar PL properties to that in solution samples.

Experimental

PS-P4VP with number average molecular weights (M_n) of PS and P4VP being 47 600 and 20 900 g/mol, respectively, and polydispersity (M_w/M_n) of 1.14, was purchased from Polymer Source. $PbCl_2$ (98%), $ZnCl_2$ (98%), Na_2S (98%) and Se powder (98%) were purchased from Aldrich. Silicon (Si) wafer was cleaned in a piranha solution (70/30 (v/v) of concentrated H_2SO_4 and 30% H_2O_2) at 80 °C for 30 min, thoroughly rinsed with deionized water, and then blown dry with nitrogen.

Synthesis of PbS (1) and PbSe (2) nanocrystals in the P4VP core of PS-P4VP block copolymer micelles

A 0.5 wt% micellar solution was prepared by dissolving the PS-P4VP block copolymer in toluene at room temperature with stirring for 3 h, then stirring for an additional 2 h at 70 °C. An excess amount of $PbCl_2$ (molar ratio of $PbCl_2$ to vinyl pyridine monomer = 60) as a precursor of PbS and PbSe nanoparticles was added to the micellar toluene solution and stirred for at least 24 h. To remove the undissolved excess amount of $PbCl_2$, the solution was filtered through a 450 nm syringe filter (Whatman, Teflon membranes) and layered on top of the freshly prepared Na_2S or NaHSe[40] aqueous solution under inert atmosphere. The molar ratio of Na_2S (or NaHSe) solution to PS-P4VP-$PbCl_2$ solution was more than ten times. The heterogeneous solution mixture was further stirred for more than 24 h at room temperature. The appearance of a dark brown color slowly in the colorless micellar solution clearly indicates the formation PbS or PbSe nanocrystals. Then the top toluene layer containing PS-P4VP-PbS (**1**) or PS-P4VP-PbSe (**2**) was carefully removed from the aqueous solution by syringe.

Post treatment of PbSe nanocrystals

The sample **2** was layered on top of the aqueous Na_2S solution and stirred for more than 12 h. Then the top toluene layer was carefully removed and stored at room temperature. This is referred to as sample **3**.

An excess amount of $ZnCl_2$ (molar ratio of $ZnCl_2$ to vinyl pyridine monomer = 50) was added to the micellar solution of sample **2** and the solution was stirred for more than 24 h. The $ZnCl_2$ was included in the P4VP core due to strong coordination with pyridine units. We have also confirmed that the reverse is not possible, i.e. the inclusion of $PbCl_2$ in the PS-P4VP-ZnS micelle core. Then the solution was filtered through a 450 nm syringe filter on top of the freshly prepared aqueous Na_2S solution and the solution mixture was further stirred for more than 12 h. The top toluene layer was finally removed and stored at room temperature; this is referred to as sample **4**. A similar experiment could not be performed on sample **1**. The dark colored solution **1** becomes slowly colorless upon addition of $ZnCl_2$ that could be either due to the complete removal of PbS nanocrystals or replacement of Pb with Zn ions.

Characterization

All characterizations were carried out after keeping the samples **1–4** for more than a month at room temperature. Monolayer thin films were fabricated by spin coating at 4000 rpm on a cleaned silicon wafer.

HR-TEM (high resolution-transmission electron microscopy) images were acquired by a JEOL JEM-2100F field emission-TEM operated at 200 kV. EDX (energy dispersive X-ray spectroscopy) spectra were obtained by Oxford Inst, INCA EDX microanalysis system implemented on the JEOL JEM-2100F HR-TEM. The samples were prepared by directly dipping the TEM grid into the micellar solution. For powder X-ray diffraction, the sample was prepared by solution casting of micellar solutions on the cleaned silicon wafer. Powder X-ray diffraction measurements were taken on a RIGAKU D-MAX1400.

UV-VIS spectra were obtained by using Carry 5000 UV-vis-near infrared double beam spectrophotometer. Photoluminescence (PL) spectra were collected with a laser excitation source instrument. The 800 nm laser beam from a continuous-wave Ti:Sapphire laser was used as an excitation source. The laser beam was focused on the sample surface through a 5 cm focusing lens, and the beam size at the focal point was ~300 μm. The PL spectra were recorded with 1/4m monochromator A combination of the monochromator (Oriel 77200), InSb (Judson SP28) or PIN detector (Thorlabs DET410), lock-in amplifier, and mechanical chopper was used to record the photoluminescence of nanocrystals while the specimens were excited continuously. Photoluminescence intensity at the emission peak was recorded every 300 ms with the integration time of 100 ms.

Thin films characterizations

The morphology of block copolymer micellar template was characterized by scanning probe microscopy (SPM) with tapping mode (Nanoscope IIIa, Digital Instruments/Veeco) and field-emission scanning electron microscopy (FE-SEM: Hitachi, S-4800) operated at 5 kV.

Results and discussions

Fig. 1 shows the TEM images and EDX spectra of samples **1** and **2**. The images clearly show the formation of PbS and PbSe nanocrystals only at the micelles core. The high magnification of the images reveals the presence of different sized multiple nanocrystals in a single micelle core (Fig. 1 b, e). The inset in the Fig. 1 (a, d) shows the HR-TEM image of the corresponding nanocrystals. The well developed lattice fringes in both samples indicate a high crystallinity of the PbS and PbSe nanoparticles. The EDX studies confirm the presence of Pb and S elements in sample **1** (Fig. 1c) and Pb and Se elements in sample **2** (Fig. 1f).

The TEM images of samples **3** and **4** are shown in Fig. 2 (a–d). The size of PbSe nanocrystals in sample **3** (Fig. 2b) appears very similar to the sample **2**. The well developed lattice fringes observed in HR-TEM indicate the good crystallinity of the

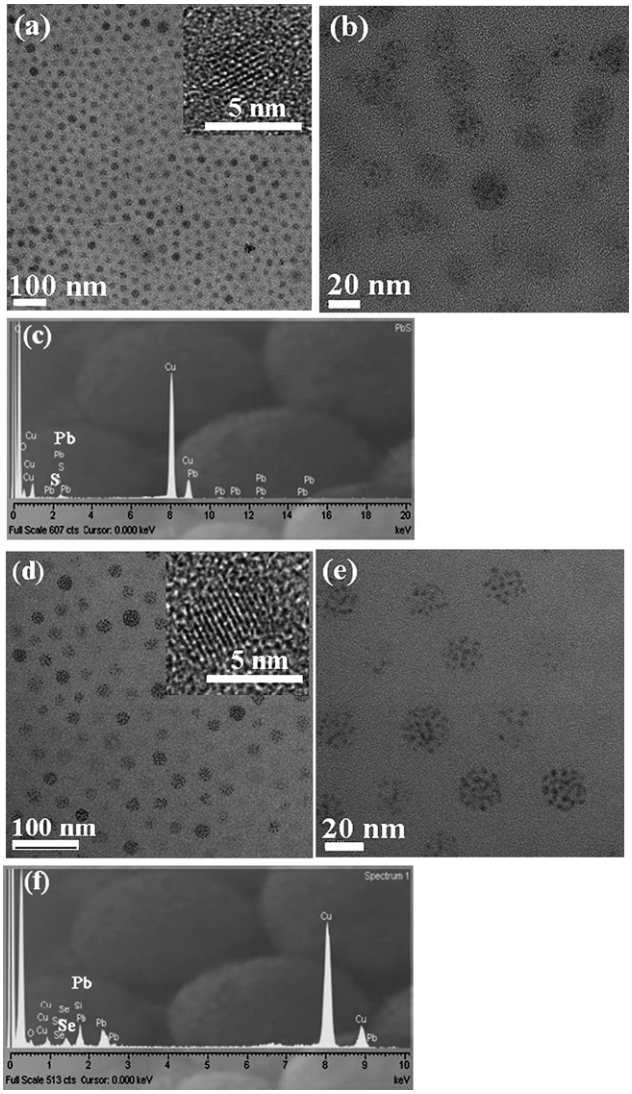

Fig. 1 TEM images of sample **1** (a, b) and sample **2** (d, e) and EDX spectra of sample **1** (c) and sample **2** (f). HR-TEM images are shown in the inset (a) and (d).

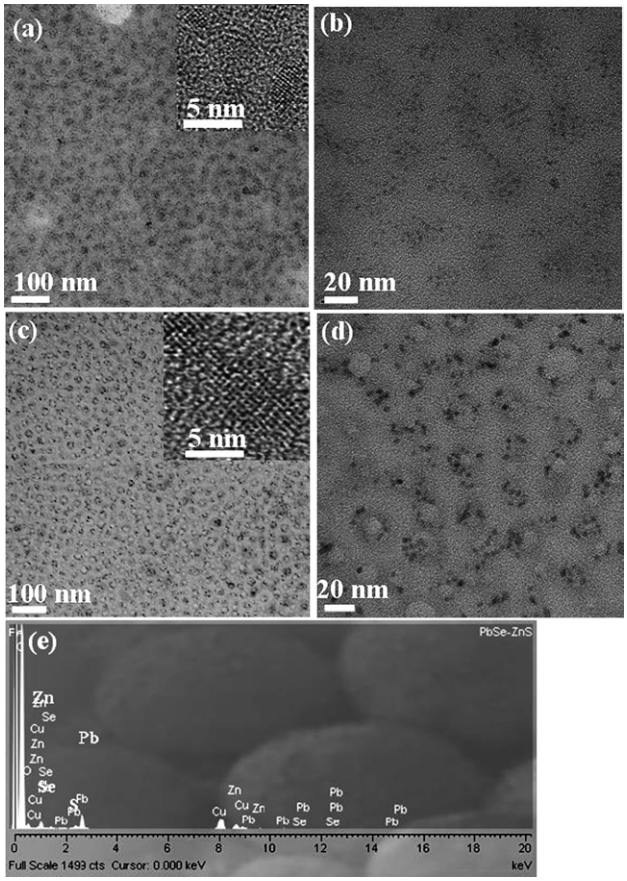

Fig. 2 TEM images of sample **3** (a, b) and sample **4** (c, d) and EDX spectrum of sample **4** (e). HR-TEM images are shown in the inset (a) and (c).

sample. The inclusion of ZnS in the P4VP core was confirmed by EDX, which shows clearly the presence of Zn and S elements along with Pb and Se (Fig 2e). The HR-TEM image as shown in the inset of Fig. 2c demonstrates the high crystallinity of the nanocrystals. PbSe nanocrystals in sample **4** appear slightly bigger and very distinct compared to samples **2** and **3**, although the reason is not clear. The size of PbSe nanocrystals in the micelles core of samples **2** and **3** is 2–3 nm, whereas that of sample **4** is 3–6 nm. The PL characteristics of the nanocrystals support the size changes in sample **4** compared to samples **2** and **3**, as well as the presence of different sized nanocrystals in the micelle core, which will be discussed in the following section.

The powder XRD patterns of samples **1–4** are shown in Fig. 3. The diffraction patterns indicate the good crystallinity of the obtained nanocrystals. The reflection peaks of sample **1** at $2\theta =$ 25.81, 30.20 and 43.08 correspond to (111), (200) and (220) planes of the face-centered cubic (fcc) rock-salt-structured PbS, which is in good agreement with the literature values (JCPDS Card No. 05-592).[41] The diffraction peaks of sample **2** at $2\theta =$ 28.85 and 41.54 correspond to the (200) and (220) planes, which can be indexed to the pure clausthalite phase of rock-salt structured PbSe (JCPDS Card No. 78-1902).[42] The diffraction peaks of sample **3** are essentially same as those of sample **2**, which indicates that the post treatment with Na_2S on PbSe nanocrystals does not change the PbSe nanocrystals. Interestingly, the powder XRD pattern of sample **4**, in which ZnS has been included in the P4VP/PbSe core, exhibits the peaks corresponding only to the PbSe structure. This indicates that ZnS is formed as an amorphous phase in the micelles core. We confirmed by a separate experiment that only an amorphous phase of ZnS was formed when only $ZnCl_2$ was incorporated into the P4VP core and converted to ZnS nanoparticles. The absence of any impurity peak in all samples reveals the high purity of the as-synthesized nanoparticles. The broadening of the peaks indicates that the crystallite size is small.

Fig. 4 shows the optical absorption spectra of samples **1–4**. Although all samples do not show any sharp absorption peaks, a large blue shift in the optical absorption cut-off was observed compared with the bulk PbS and PbSe materials (3020 nm for PbS and 4275 nm for PbSe).[43,44] It is noted that PS-P4VP block copolymer is transparent in the spectral range considered here. TEM investigation revealed that samples **1–3** contain nanoparticles of 2–3 nm and sample **4** contains nanoparticles of 3–6 nm. The samples **1** and **2** show an absorption edge

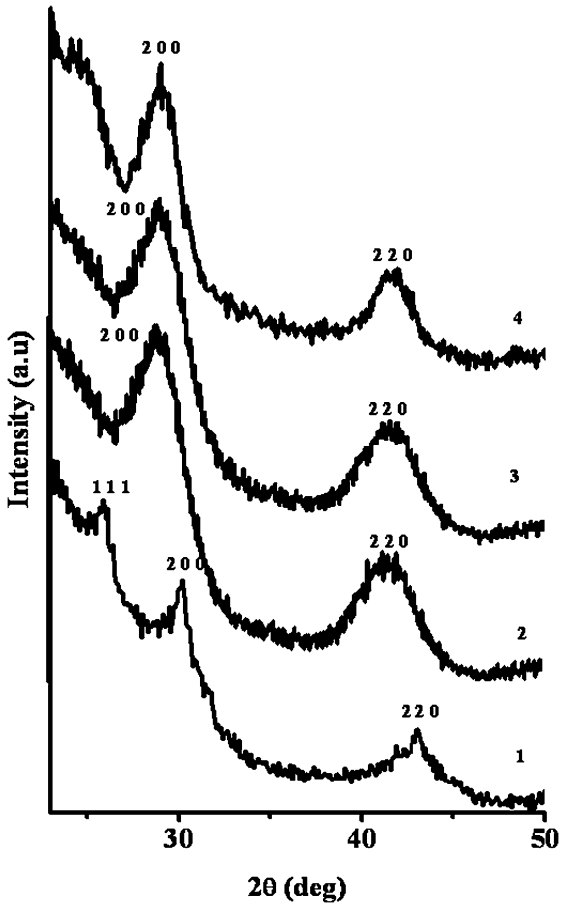

Fig. 3 Powder X-ray diffraction patterns of samples **1–4**.

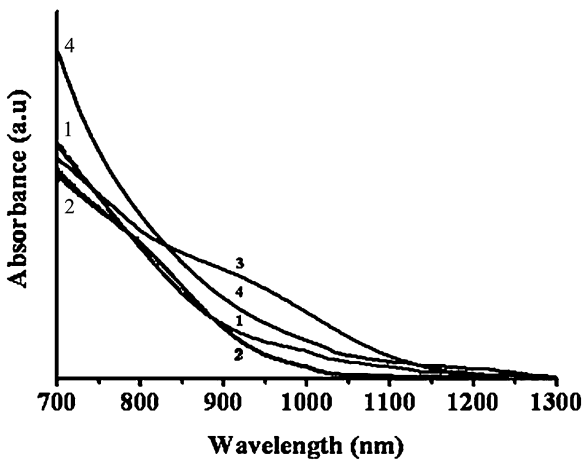

Fig. 4 Optical absorption spectra of samples **1–4** measured in solution.

corresponding to the nanoparticle size observed from TEM,[1,45] Although sample **3** contains similar particle size of **2**, it shows a slight red shift in the absorption edge. This could be due to the formation of a PbSeS alloy layer on the surface of PbSe nanocrystals. The sample **4** also exhibits a red shift in the absorption edge due to the formation of slightly bigger nanocrystals (Fig. 2d).[45]

The PL spectra of the samples **1–4** are shown in Fig. 5. The excitation at 800 nm leads to weak broad emission between

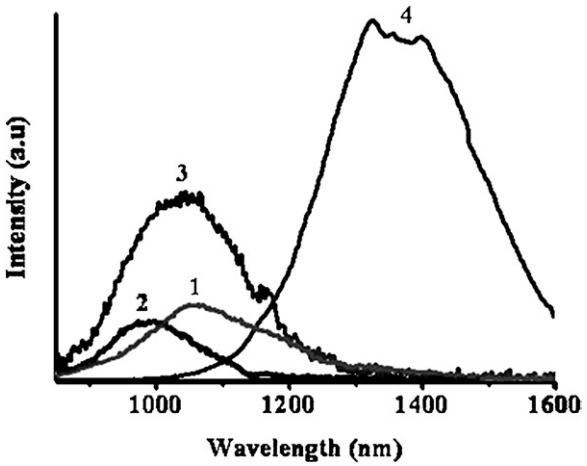

Fig. 5 Photoluminescence spectra of samples **1–4** measured in solution by exciting at 800 nm.

1000–1150 nm for sample **1**, and sample **2** also exhibits a similarly weak broad emission centered at 1000 nm. However, samples **3** and **4** show good enhancement in the emission but the peak position is slightly red shifted in sample **3**, and largely red shifted in sample **4** compared with sample **2**. The post treatment of PbSe nanocrystals with Na_2S might lead to the formation of a PbSeS alloy which might act as a surface passivation layer on the surface of PbSe nanocrystals. The formation of surface passive layer could be responsible for the enhancement of the emission intensity. Lifshitz *et al*[46] recently reported the formation of unique $PbSe/PbSe_xS_{1-x}$ core-shell nanocrystals with a tunable

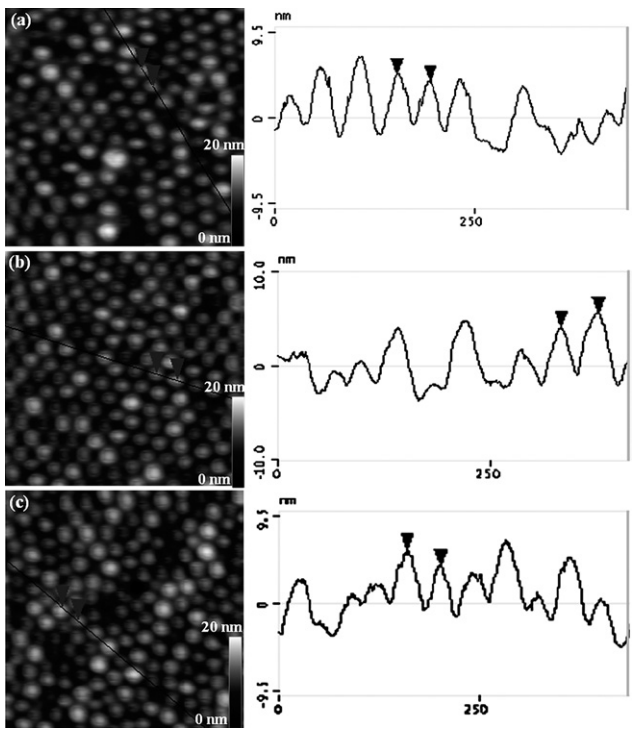

Fig. 6 SPM height images of monolayer thin films fabricated by spin coating on silicon wafer from sample **1** (a), sample **2** (b) and sample **4** (c). Image size: 500 × 500 nm.

composition of the alloyed shell showing exceptionally high luminescence quantum efficiency. Similar to sample **2**, sample **3** exhibits broad emissions centered at 1050 nm. Sample **4** shows a large red shift in the peak position, and a strong broad emission at 1300–1480 nm. This large red shift of the peak position could be due to the formation of slightly bigger nanocrystals, which is evident from the TEM images (Fig. 2d).

The synthesis of PbS and PbSe nanocrystals in the block polymer micelles offers easy fabrication of thin films by spin or dip coating on a solid substrate with selective positioning of the nanocrystals. For the thin films fabrication, we fabricated monolayer thin films by spin coating on a silicon wafer from samples **1**, **2** and **4**. Fig. 6 shows the SPM height images and cross-sectional height profiles of the fabricated monolayer thin films. The fabricated monolayer films clearly show 2-D arrays of micellar structure with selective location of nanocrystals in the micelles core. We previously reported that the average height contrast between PS matrix and P4VP domain and the domain diameter of P4VP in neat PS-P4VP monolayer film are 3 nm and 23 nm, respectively.[38] The inclusion of PbS or PbSe nanocrystals in the P4VP domain increases the diameter to 30 nm with 7 nm height contrast between PS matrix and P4VP domain for all the films. The interdomain distance (43 nm) of the monolayer films fabricated from all samples is nearly the same as that of the neat PS-P4VP monolayer film (40 nm).[38] Fig. 7 shows the FE-SEM images of thin films, which also shows 2-D arrays of monolayer structures similar to those observed by SPM.

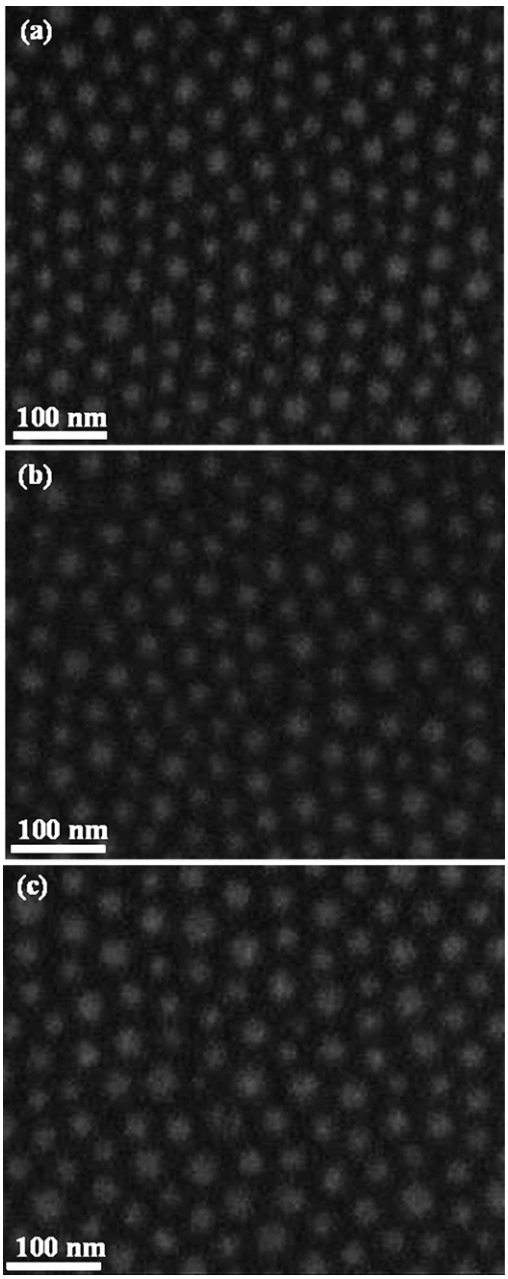

Fig. 7 FE-SEM images of monolayer thin films fabricated by spin coating on silicon wafer from sample **1** (a), sample **2** (b) and sample **4** (c).

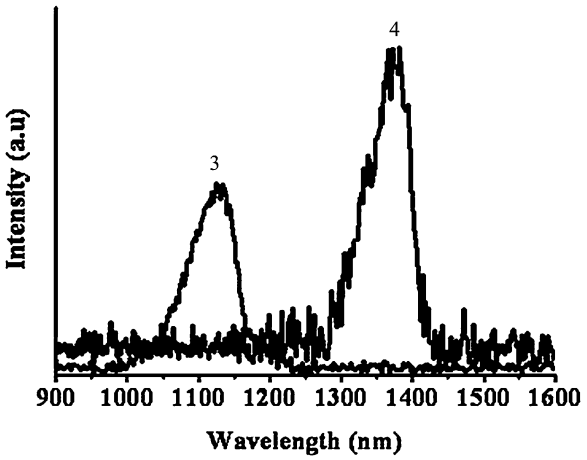

Fig. 8 Photoluminescence spectra of monolayer thin films fabricated by spin coating on silicon wafer from samples **3** and **4**.

Finally, we measured the PL for the monolayer thin films by exciting at 800 nm. The thin films fabricated from samples **1** and **2** did not show any measurable PL intensity. This is understandable since the PL emission from the bulk solution itself is very weak. However, monolayer thin films fabricated from samples **3** and **4** show distinct PL emissions, as shown in Fig. 8. Although the emission profiles of the thin films are very similar to those of solution samples, the intensity of the peak varies. Sample **3** in solution shows a broad emission centred at 1050 nm, whereas the thin film exhibits a strong peak at 1120 nm. Sample **4** in solution exhibits a broad emission maximum between 1300–1480 nm, whereas the thin film shows a clear emission peak at 1380 nm. The emission from the solution sample is the average response from all particle sizes, whereas in thin films, the peak intensity depends on the population of particular sizes of the nanocrystals available in a specific area where the incident beam is focused. This could be the reason for shifting the peak position in the thin films.

Conclusion

We have presented the direct preparation of PbS and PbSe nanocrystals at the core of the PS-P4VP micelles at room temperature. HR-TEM and X-ray diffractogram studies showed the crystalline characteristics of the nanocrystals. Optical absorption and photoluminescence studies of the nanocrystals

showed the quantized phenomena. We have shown the enhancement of the emission intensity by surface modification of the PbSe nanocrystals by post treatment with Na_2S. The inclusion of amorphous ZnS nanoparticles in the micelle core containing PbSe nanoparticles leads to the enhancement in PL intensity as well as a large red shift in the peak, which falls in the technologically important spectral range (1.3 to 1.55 μm). We also fabricated thin films of micellar structures containing nanoparticles on a solid substrate, which showed selective positioning of the nanocrystals. The PL of the thin films shows similar features to the solution samples.

Acknowledgements

This work was supported by the National Creative Research Initiative Program by KOSEF.

References

1 E. H. Sargent, *Adv. Mater.*, 2005, **17**, 515.
2 A. L. Rogach, A. Eychmüller, S. G. Hickey and S. V. Kershaw, *Small*, 2007, **4**, 536.
3 B. L. Wehrenberg, C. Wang and P. Guyot-Sionnest, *J. Phys. Chem. B*, 2002, **106**, 10634.
4 H. Du, C. Chen, R. Krishnan, T. D. Krauss, J. M. Harbold, F. W. Wise, M. G. Thomas and J. Silcox, *Nano Lett.*, 2002, **2**, 1321.
5 J. F. Peterson and T. D. Krauss, *Nano Lett.*, 2006, **6**, 510.
6 D. V. Talapin and C. B. Murray, *Science*, 2005, **310**, 86.
7 R. D. Schaller, M. A. Petruska and V. I. Klimov, *J. Phys. Chem. B*, 2003, **107**, 13765.
8 E. Lifshitz, M. Brumer, A. Kigel, A. Sashchiuk, M. Bashouti, M. Sirota, E. Galun, Z. Burshtein, A. Q. Le Quang, I. Ledoux-Rak and J. Zyss, *J. Phys. Chem. B*, 2006, **110**, 25356.
9 G. Konstantatos, I. Howard, A. Fischer, S. Hoogland, J. Clifford, E. Klem, L. Levina and E. H. Sargent, *Nature*, 2006, **442**, 180.
10 S. A. Mcdonald, G. Konstantanos, S. Zhang, P. W. Cyr, E. J. D. Klem, L. Levina and E. H. Sargent, *Nat. Mater.*, 2005, **4**, 138.
11 M. Böberl, M. V. Kovalenko, S. Gamerith, E. List and W. Heiss, *Adv. Mater.*, 2007, **19**, 3574.
12 J. S. Steckel, S. Coe-Sullivan, V. Bulovic and M. G. Bawendi, *Adv. Mater.*, 2003, **15**, 1862.
13 M. S. Dresselhaus, G. Chen, M. Y. Tang, R. Yang, H. Lee, D. Wang, Z. Ren, J. -P. Fleurial and P. Gogna, *Adv. Mater.*, 2007, **19**, 1043.
14 M. Chen, Y. Xie, J. C. Lu, Y. J. Zhu and Y. T. Qian, *J. Mater. Chem.*, 2001, **11**, 518.
15 G. R. J. Ellingson, M. C. Beard, J. C. Johnson, P. Yu, O. I. Micic, A. J. Nozik, A. Shabaev and A. L. Efros, *Nano Lett.*, 2005, **5**, 865.
16 M. V. Kovalenko, E. Kaufmann, D. Pachinger, J. Roither, M. Huber, J. Stangl, G. Hesser, F. Schaffler and W. Heiss, *J. Am. Chem. Soc.*, 2006, **128**, 3516.
17 J. M. Pietryga, R. D. Schaller, D. Werder, M. H. Stewart, V. I. Klimov and J. A. Hollingsworth, *J. Am. Chem. Soc.*, 2004, **126**, 11752.
18 M. J. Ventura and M. Gu, *Adv Mater.*, 2008, **20**, 1329.
19 C. Lu, C. Guan, Y. Liu, Y. Cheng and B. Yang, *Chem. Mater.*, 2005, **17**, 2448.
20 P. Schuetz and F. Caruso, *Chem. Mater.*, 2004, **16**, 3066.
21 A. K. Dutta, T. Ho, L. Zhang and P. Stroeve, *Chem. Mater.*, 2000, **12**, 1042.
22 Y. Zhou, H. Itoh, T. Uemura, K. Naka and Y. Chujo, *Langmuir*, 2002, **18**, 5287.
23 W. P. Lim, H. Y. Low and W. S. Chin, *J. Phys. Chem. B.*, 2004, **108**, 13093.
24 J. Kuljanin, M. I. Comor, V. Djoković and J. M. Nedeljković, *Mater. Chem. Phys.*, 2006, **95**, 67.
25 X. Lu, X. Y. Zhao and C. Wang, *Adv. Mater.*, 2005, **17**, 2485.
26 T. Cui, F. Cui, J. Zhang, J. Wang, J. Huang, C. Lu, Z. Chen and B. Yang, *J. Am. Chem. Soc.*, 2006, **128**, 6298.
27 S. Förster and T. Plantenberg, *Angew. Chem., Int. Ed.*, 2002, **41**, 688.
28 I. W. Hamley, *Nanotechnology*, 2003, **14**, R39.
29 S. I. Yoo, J. H. Kwon and B. H. Sohn, *J. Mater. Chem.*, 2007, **17**, 2969.
30 Q. Zhang, S. Gupta, T. Emrick and T. P. Russell, *J. Am. Chem. Soc.*, 2006, **128**, 3898.
31 C. -P. Li, S. -W. Yeh, H. -C. Chang, J. Y. Huang and K. -H. Wei, *Small*, 2006, **2**, 359.
32 S. Zou, R. Hong, T. Emrick and G. C. Walker, *Langmuir*, 2007, **23**, 1612.
33 M. Moller and J. Spatz, *Curr. Opin. Colloid Interface Sci.*, 1997, **2**, 177.
34 H. Yusuf, W. -G. Kim, D. H. Lee, M. Aloshyna, A. G. Brolo and M. G. Moffitt, *Langmuir*, 2007, **23**, 5251.
35 Y. Martinez, J. Retuert, M. Yazdani-Pedram and H. Cölfen, *J. Mater. Chem.*, 2007, **17**, 1094.
36 L. Qi, H. Cölfen and M. Antonietti, *Nano Lett.*, 2001, **1**, 61.
37 K. D. Gatsouli, S. Pispas and E. I. Kamitsos, *J. Phys. Chem. C*, 2007, **111**, 15201.
38 J. K. Kim, J. I. Lee and D. H. Lee, *Macromol. Res.*, 2008, **16**, 267.
39 S. P. Anthony and J. K. Kim, *Chem. Commun.*, 2008, 1193.
40 D. L. Klayman and T. S. Griffin, *J. Am. Chem. Soc.*, 1973, **95**, 197.
41 Y. -H. Zhang, L. Guo, P. -G. Yin, R. Zhang, Q. Zhang and S. -H. Yang, *Chem. Eur. J.*, 2007, **13**, 2903.
42 J. Zhu, S. T. Aruna, Y. Koltypin and A. Gedanken, *Chem. Mater.*, 2000, **12**, 143.
43 P. Zhao, J. Wang, G. Cheng and K. Huang, *J. Phys. Chem. B.*, 2006, **110**, 22400.
44 E. A. Streltov, N. P. Osipovich, L. S. Ivashkevich, A. S. Lyakhov and V. V. Sviridov, *Electrochim. Acta*, 1998, **43**, 869.
45 M. V. Kovalenko, D. V. Talapin, M. A. Loi, F. Cordella, G. Hesser, M. I. Bodnarchuk and W. Heiss, *Angew. Chem., Int. Ed.*, 2008, **47**, 3029.
46 M. Brumer, A. Kigel, L. Amirav, A. Sashchiuk, O. Solomesch, N. Tessler and E. Lifshitz, *Adv. Funct. Mater.*, 2005, **15**, 1111.